Available online at www.sciencedirect.com
SCIENCE DIRECT®
Journal of Solid State Chemistry 177 (2004) 2961–2970
JOURNAL OF SOLID STATE CHEMISTRY
http://elsevier.com/locate/jssc

Structural investigation of trimethylammonium tetrachloromercurate

M. Amami,[a,b] Sander van Smaalen,[a,*] A. Ben Salah,[b] Xavier Helluy,[c] and Angelika Sebald[c]

[a] *Laboratory of Crystallography, University of Bayreuth, 95440 Bayreuth, Germany*
[b] *Laboratory of Material Sciences and Environment, University of Sfax, 3038 Sfax, Tunisia*
[c] *Bayerisches Geoinstitut, University of Bayreuth, 95440 Bayreuth, Germany*

Received 9 February 2004; received in revised form 23 April 2004; accepted 2 May 2004

Abstract

The temperature dependence of the crystal structure of $TrMA_2HgCl_4$ (TrMA = trimethylammonium) is studied by single-crystal and powder X-ray diffraction between 161 and 373 K. Below room temperature, we did not find significant changes of the crystal structure. The phase transition at 325 K is described by a rotation of one of the two independent $TrMA^+$ cations by 40° around the N–H axis, resulting in major rearrangements in the network of hydrogen bonds. A large change of the volume of the unit cell is found at the phase transition at 357 K, resulting in damage to the single crystals. Powder diffraction then shows that this transition can be described as a α–β transition between the α and β-K_2SeO_4 structure types. Structure refinements employing alternatively restrictions by the space group and additional restrictions by the C_3 non-crystallographic site symmetry for the $TrMA^+$ cations show that significant deviations from C_3 symmetry of the $TrMA^+$ cations do not exist at any temperature. The molecular dynamics and orientational disorder were studied by the maximum entropy method applied to the X-ray data. The diffraction results are corroborated by temperature dependent NMR experiments.

Keywords: Trimethylammonium; X-ray diffraction; Phase transitions

1. Introduction

Alkylammonium tetrachlorometallates, with the general formula A_2MCl_4 (A = alkylammonium ion; M = divalent metal), have been widely investigated owing to their interesting physical properties connected to the various phase transitions. The nature of the complicated phase transitions in these mixed organic–inorganic salts could be related to either an annealing of the crystal structure with intrinsic disorder of the alkylammonium and MX_4^{2-} groups or a reorientation of the organic cation and thus to changes in the network of hydrogen bonds [1–5]. The existence of C–H···Cl hydrogen bonds has been recently reviewed by Aakeroey et al. [6] through a systematic data mining and statistical analysis of the Cambridge structural database [7]. The MX_4^{2-} anions in organic inorganic hybrid solids are capable of participating in C–H···Cl as well as N–H···Cl hydrogen bonds with organic cations. The importance of this type of hydrogen bonding is now well established in crystal engineering and in the supramolecular architectures of organic species, as well as in biomolecular structures and transition metal complexes [8].

The crystal structure of trimethylammonium tetrachloromercurate (II) ($TrMA_2HgCl_4$) was studied at room temperature by Ben Salah et al. [9]. They found a fully ordered structure comprising of $[NH(CH_3)_3]^+$ ($TrMA^+$) cations and $[HgCl_4]^{2-}$ anions. Each of the two crystallographically independent $TrMA^+$ cations was reported to be involved in a single hydrogen bond N–H···Cl towards a single chlorine atom.

Previously we have reported the structure at 343 K [10]. Although the symmetry was the same as at room temperature, major rearrangements of the framework of hydrogen bonds were found. This could be correlated to an anomalously large increase of the lattice parameter *a* between 310 and 330 K, and we have interpreted these features as a non-symmetry breaking phase transition at a temperature of 325 K.

*Corresponding author. Fax: +49-921-553770.
E-mail address: smash@uni-bayreuth.de (S. van Smaalen).

0022-4596/$ - see front matter © 2004 Elsevier Inc. All rights reserved.
doi:10.1016/j.jssc.2004.05.012

Here we report differential scanning calorimetry (DSC) measurements between 100 and 400 K, which indicate the existence of four phase transitions. Furthermore, we have extended our X-ray diffraction studies towards lower and higher temperatures, in order to obtain a complete picture of the structural changes at the phase transitions in $TrMA_2HgCl_4$. The orientational order of the three crystallographically independent complex ions is studied by the maximum entropy method (MEM) [11].

2. Experimental

2.1. Thermal analysis

Differential scanning calorimetry (DSC) was measured on a Shimadzu instrument with Al_2O_3 as reference material. The samples were loaded into alumina crucibles, and kept in a flow of nitrogen gas. DSC was measured in the temperature range 100–400 K with heating and cooling rates of 5 K/min. About 10 mg of sample were used for each run. The trace for $TrMA_2HgCl_4$ is given in Fig. 1. A large anomaly is observed at 357 K on heating and at 304 K on cooling, indicating a first-order phase transition with a hysteresis of 53 K. Three other anomalies are seen in this figure, indicating three further phase transitions at lower temperatures.

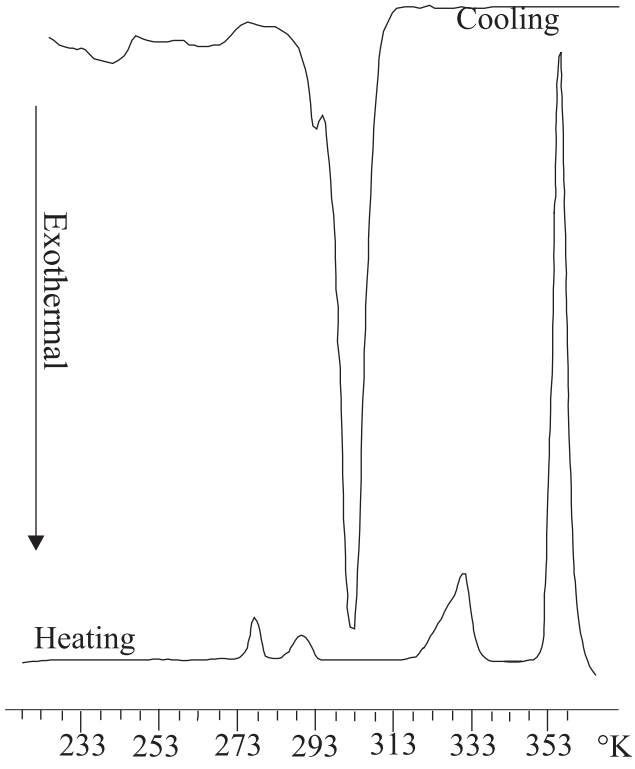

Fig. 1. DSC trace on heating and cooling for an as grown sample of $TrMA_2HgCl_4$.

2.2. X-ray diffraction

Single crystal X-ray diffraction at low temperatures was measured with a Nonius MACH3 diffractometer equipped with a rotating anode generator and Mo$K\alpha$ radiation. Lattice parameters were determined at selected temperatures between 160 and 290 K. They were obtained from the setting angles of 25 reflections in the range $8.9° < 2\theta < 27.7°$. A smooth temperature dependence of the monoclinic lattice parameters is found without indications for anomalies or phase transitions (Fig. 2).

At a temperature of 161 K, integrated intensities were measured by $\omega - 2\theta$ scans of all Bragg reflections up to $2\theta = 60°$. The data were corrected for the variations of the intensities of three standard reflections, and the Lorentz and polarization effects, employing the computer program HELENA [12]. The absorption correction was calculated from the crystal shape, as it was determined by refinements against ψ-scans using the computer program HABITUS [13]. Further experimental details are given in Table 1.

Single-crystal X-ray diffraction at high temperatures was measured with synchrotron radiation at beamline F1 of HASYLAB at DESY (Hamburg), using a Huber four-circle Kappa diffractometer equipped with a Siemens SMART CCD area detector. A double-crystal Si(111) monochromator was used to select a wavelength of $\lambda = 0.5000$ Å. Rotation images were measured with a step width of 0.01° in ω. Several runs were made for different settings of the ϕ and χ angles. Data processing was performed with the SMART and SAINT software [14]. The data were empirically corrected for absorption and other effects (absorption by air, glue and glass capillary) using SADABS [15]. Complete data sets were obtained at temperatures of 343 K (see [10]) and 295 K.

For all three data sets, the systematic extinctions were found to be in accordance with the space group $P2_1/n$. Structure refinements were performed by full-matrix least squares on F^2 using SHELXL97 [16] and

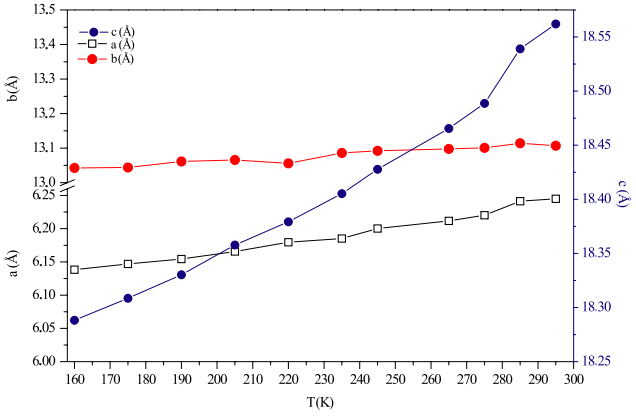

Fig. 2. Temperature dependence of the lattice parameters of $TrMA_2HgCl_4$.

Table 1
Experimental data

Temperature (K)	161	295
Crystal data		
Chemical formula	$[NH(CH_3)_3]_2HgCl_4$	$[NH(CH_3)_3]_2HgCl_4$
Chemical formula weight	462.6	462.6
Cell setting	Monoclinic	Monoclinic
Space group	$P2_1/n$	$P2_1/n$
a (Å)	18.360(2)	18.561(2)
b (Å)	6.164(2)	6.245(2)
c (Å)	13.070(2)	13.106(2)
γ (deg)	92.20(1)	92.00(1)
Z	4	4
D_x (Mg m^{-3})	2.078	2.023
Radiation type	Mo$K\alpha$	Synchrotron
Wave length (Å)	0.71073	0.5000
μ (mm^{-1})	11.10	4.38
Crystal form	Polyhedron	Polyhedron
Crystal size (mm^3)	$0.06 \times 0.035 \times 0.025$	$0.07 \times 0.11 \times 0.05$
Crystal colour	Colourless	Colourless
Data collection		
Diffractometer	Nonius-MACH3	Huber–Kappa
Data collection method	ω-2θ-scan	ω-scan
Absorption correction	ψ-scan	SADABS
T_{min}	0.182	0.501
T_{max}	0.324	0.695
No. of independent reflection	2148	2140
No. of observed reflections	1769	1992
Criterion of observability	$I > 3\sigma(I)$	$I > 2\sigma(I)$
R_{int}	0.056	0.0648
θ_{max} (deg)	29	16.18
Range of h, k, l	$-25 < h < 25$	$0 < h < 20$
	$0 < k < 8$	$-6 < k < 6$
	$0 < l < 18$	$0 < l < 14$
Refinement		
Refinement on	F	F
R	0.0668	0.0287
wR_{F^2}	0.0885	0.0424
No. of parameters	119	119
Weighting scheme	$[\sigma^2(F) + (0.02F)^2]^{-1}$	$[\sigma^2(F) + (0.015F)^2]^{-1}$
$\Delta\rho_{max}$ (eÅ^{-3})	6.2	0.65
$\Delta\rho_{min}$ (eÅ^{-3})	−6.8	−0.69
Extinction correction	Isotropic type I (Becker & Coppens, 1974)	
Extinction coefficient	0.07 (2)	0.16 (4)
Atomic scattering factors	International Tables for Crystallography	
	Vol. C (1992)	

JANA2000 [17]. Anisotropic temperature factors were used for the non-hydrogen atoms. Hydrogen atoms were included at calculated positions, and they were given isotropic temperature factors.

An attempt to measure single-crystal X-ray diffraction in the high-temperature phase ($T > 358$ K) was made with the CCD detector at beamline F1 of Hasylab. For two specimens we found that the crystal was damaged at the transition, resulting in multiply split reflections and partial powder rings on the area detector. These features can be related to the first-order character of the transition and the jump in the volume of the unit cell [10], apparently causing such a large strain that the crystal was damaged. They prohibited the extraction of a data set of integrated Bragg reflections from the measured images.

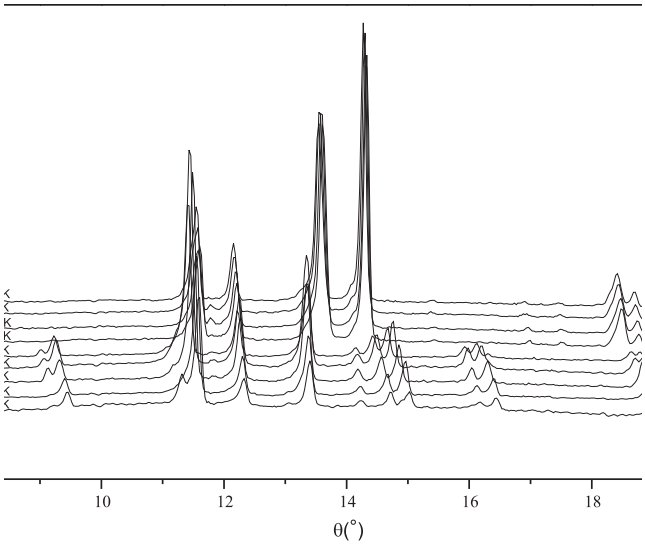

Fig. 3. X-ray powder diffraction diagrams at different temperatures between 295 and 373 K. A first-order phase transition is clearly visible between 333 and 343 K.

As an alternative, we turned to X-ray powder diffraction to study the high-temperature phase transition. X-ray powder diffraction was measured at several temperatures between 295 and 373 K using a Nonius PDS120 diffractometer equipped with a curved position sensitive detector and a graphite monochromator to select the Cu$K\alpha_1$ radiation ($\lambda = 1.5418$ Å). The samples were loaded into capillaries, that were spun during the measurements, in order to improve randomization of the crystallites. Data were taken at room temperature in continuous scanning mode for several hours. An additional phase was observed, which was identified as $TriMA_2HgCl_3$. Data reduction, including the determination of a manual background, was performed using the computer program GUFI [18]. Inspection of the diffraction diagrams clearly show the structural character of the high-temperature phase transition by the disappearance of many reflections between 333 and 343 K (Fig. 3). The mismatch in temperatures between the synchrotron experiment and the powder diffraction probably is due to difficulties in measuring the precise temperature at the sample in the powder diffraction experiments.

2.3. NMR experiments

Nuclear magnetic resonance (NMR) experiments were carried out on a Bruker MSL 300 spectrometer,

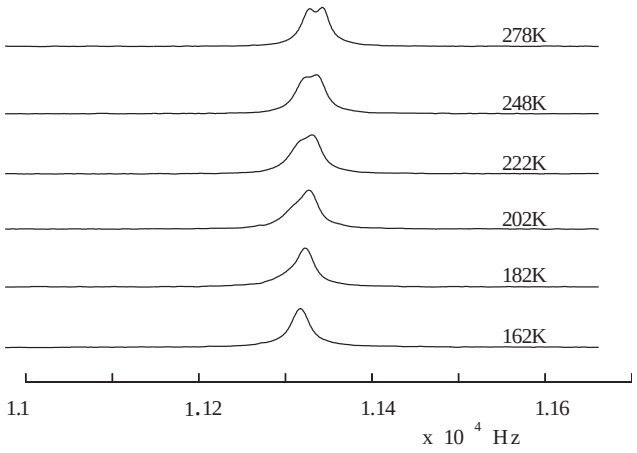

Fig. 4. ^{13}C NMR spectra at selected temperatures between 160 and 280 K. Additional spectra up to 350 K (not shown) indicate a smooth temperature dependence of the positions of the resonances. The experimental parameters are: 12 scans accumulated for each spectrum, CP contact time 5 ms, recycle delays 8 s, ^{1}H decoupling strength 50 kHz, MAS frequency 2 kHz.

corresponding to the ^{13}C Larmor frequency of 75.5 MHz. The sample consisted of about 1100 mm^3 of pulverized single crystals loaded into a standard 7 mm rotor made of zirconia with a boron nitride end cap. Standard ^{13}C cross polarization (CP) magic-angle spinning (MAS) experiments [19] were performed at 32 different temperatures between 140 and 350 K (Fig. 4). Waiting periods for temperature equilibration between variable-temperature experiments of 10–20 min were chosen.

The most obvious result is that the NMR spectra exhibit two resonances at all temperatures between 200 and 350 K, while they merge into a single broad peak below 182 K (Fig. 4). This indicates the presence of two carbon atoms with slightly different environments. Consequently the NMR is in agreement with both crystallographically independent $TrMA^+$ ions having threefold symmetry. Unfortunately, this result implies that different states of dynamic disorder of the $TrMA^+$ ions cannot be distinguished by the NMR. Phase transitions cannot be deduced from the gradual temperature dependence of the NMR, but, as stated above, transitions involving a change of the dynamics of the $TrMA^+$ ions would not be visible in the recorded spectra.

3. Structure refinements

3.1. The structure at 295 K

Refinements of the structure at 295 K were performed with the ordered structure reported by Ben Salah et al. [9] as a start model. Refinement of the coordinates and temperature parameters of all crystallographically independent atoms resulted in a good fit to the diffraction data with $R = 0.0278$ and $wR = 0.0424$. This structure model is referred to as M_{ord} (Table 2).

Table 2
Relative atomic coordinates and equivalent isotropic thermal parameters ($Å^2$) for the model M_{ord} at 295 K

	x	y	z	U_{iso}
Hg	0.34417(1)	0.26782(3)	0.25669(2)	0.0543(1)
Cl1	0.34289(9)	0.6787(2)	0.26104(8)	0.0567(5)
Cl2	0.40269(8)	0.1836(2)	0.09556(10)	0.0688(5)
Cl3	0.42571(8)	0.1810(2)	0.39966(10)	0.0681(5)
Cl4	0.21901(8)	0.1546(3)	0.28223(14)	0.0793(6)
N1	0.4871(3)	0.1750(9)	0.7660(3)	0.0604(17)
H1	0.5328	0.131	0.7605	0.074708
N2	0.7836(3)	0.2991(8)	0.0139(3)	0.082(2)
H2	0.799	0.3378	0.0768	0.097888
C1	0.4693(3)	0.2890(12)	0.6727(5)	0.082(2)
H1a	0.5022	0.4108	0.6657	0.123474
H1b	0.421	0.3374	0.6773	0.123474
H1c	0.4738	0.1959	0.6157	0.123474
C2	0.4835(4)	0.3136(13)	0.8547(5)	0.101(3)
H2a	0.4969	0.2342	0.9141	0.158734
H2b	0.4353	0.3608	0.8621	0.158734
H2c	0.5161	0.4334	0.8452	0.158734
C3	0.4396(5)	−0.0177(12)	0.7798(6)	0.094(3)
H3a	0.4515	−0.0847	0.8435	0.145762
H3b	0.4475	−0.115	0.7249	0.145762
H3c	0.3906	0.0228	0.7808	0.145762
C4	0.7764(4)	0.4945(10)	−0.0452(5)	0.095(3)
H4a	0.8219	0.5637	−0.0551	0.146699
H4b	0.7443	0.5868	−0.0103	0.146699
H4c	0.7552	0.4574	−0.1113	0.146699
C5	0.7154(5)	0.1833(17)	0.0251(7)	0.166(5)
H5a	0.6806	0.281	0.0535	0.246448
H5b	0.7198	0.0651	0.0691	0.246448
H5c	0.698	0.1373	−0.0408	0.246448
C6	0.8402(7)	0.1686(14)	−0.0327(7)	0.174(6)
H6a	0.8841	0.2535	−0.0373	0.254863
H6b	0.8252	0.1221	−0.0989	0.254863
H6c	0.8478	0.0461	0.0102	0.254863

Standard uncertainties are given in parentheses.

A second structure model was developed, that imposed 3-fold symmetry on the $TrMA^+$ complex ions (point group C_3). The $TrMA^+$ group was defined by the atom N in the origin of a Cartesian coordinate system, the atom H on the 3-fold axis along $(0, 0, 1)$ at a fixed distance of 0.97 Å from the nitrogen atom, and a single independent C atom on $(x, 0, z)$. The two other C atoms were generated by the 3-fold symmetry. Two internal coordinates were refined (the parameters x and z of the C atom), that completely define the shape of the $TrMA^+$ ion. The hydrogen atoms of the methyl groups were modelled by an increased occupancy of the C atoms (final refined value 1.1). The two crystallographically independent $TrMA^+$ ions were obtained by the refinement of independent positions and orientations of two copies of the $TrMA^+$ group defined above. This description results in a total of 14 positional parameters for the two $TrMA^+$ groups as compared to

24 crystallographically independent positional parameters of the 8 non-hydrogen atoms in M_{ord}. An even larger reduction is obtained for the number of independent temperature parameters. The refinement of the model M_{C3} again resulted in a good fit with $R = 0.0376$ and $wR = 0.0585$ (Table 3 and Fig. 5).

Table 3
Atomic coordinates and equivalent isotropic thermal parameters for the model M_{C3} at 295 K

	x	y	z	U_{iso} (Å^2)
Hg	0.34418(2)	0.26787(4)	0.25671(2)	0.05387(19)
Cl(1)	0.3429(1)	0.6789(3)	0.2610(1)	0.0563(7)
Cl(2)	0.4028(1)	0.1841(3)	0.0954(1)	0.0679(6)
Cl(3)	0.4255(1)	0.1810(3)	0.3997(1)	0.0674(7)
Cl(4)	0.2189(1)	0.1546(4)	0.2817(2)	0.0791(8)
Trimethylammonium molecular cation				
N(1)	0.0	0.0	0.0	0.066(1)
H(1)	0.0	0.0	0.074	0.11(2)
C(1)	0.0762(2)	0.0	−0.0334(5)	0.120(2)
	φ	χ	ψ	
TrMA(1)	72.6(4)	95.6(3)	−65.9(2)	
TrMA(2)	134.9(8)	23.0(3)	−43.8(7)	
	X_0	Y_0	Z_0	
TrMA(1)	0.4873(3)	0.1751(8)	0.7672(3)	
TrMA(2)	0.7850(2)	0.3008(6)	0.0129(4)	

The atoms N(1), H(1) and C(1) define the $TrMA^+$ group with N(1) at the origin of the coordinate system, and H(1) along $(0,0,1)$ on the internal 3-fold axis. TrMA(i) $(i = 1,2)$ are the two independent $TrMA^+$ molecules at positions (X_0, Y_0, Z_0) and with orientations described by (φ, χ, ψ). Standard uncertainties are given in parentheses.

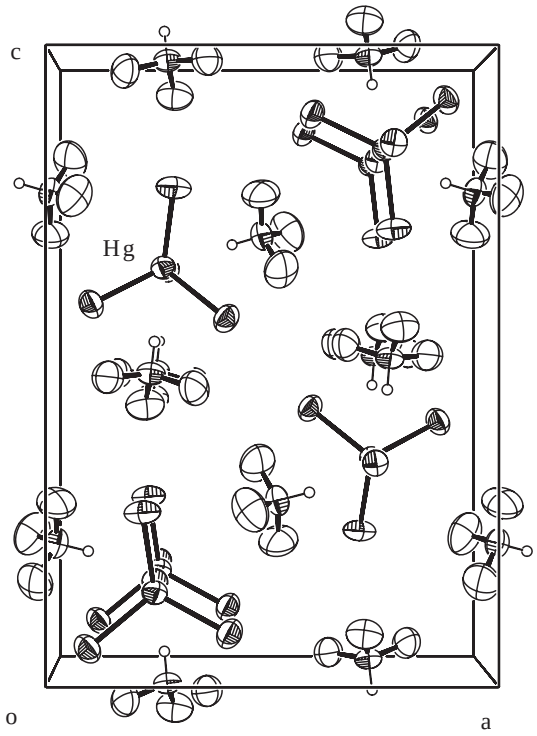

Fig. 5. Perspective view along **b** of the crystal structure at 295 K. Displacement ellipsoids are shown at 50% probability level (Ortep).

3.2. *The structure at* 161 K

Refinements of the structure at 161 K were performed within the models M_{C3} and M_{ord}. In both cases the corresponding structure at room temperature was used as start model. Reasonable fits to the diffraction data were obtained with $R = 0.0692$ for M_{C3} and $R = 0.0668$ for M_{ord} (Tables 4 and 5). The poorer quality of the fit at 161 K than at room temperature was due to instrumental instabilities during the experiment. However, it was established that the temperature was constant at 161 K.

3.3. *The structure at* 343 K

In a previous paper [10] we have reported the crystal structure of the $TrMA_2HgCl_4$ at 343 K as obtained by refinements in the model M_{C3}. The difference between the structures at 295 and 343 K was found to be major

Table 4
Atomic coordinates and equivalent isotropic thermal parameters for the model M_{ord} at 161 K

	x	y	z	U_{eq} (Å^2)
Hg	0.34402(3)	0.26701(8)	0.25905(4)	0.02670(16)
Cl1	0.3427(2)	0.6810(5)	0.2635(3)	0.0308(9)
Cl2	0.4019(2)	0.1802(6)	0.0967(3)	0.0329(10)
Cl3	0.4310(2)	0.1795(6)	0.3998(2)	0.0295(9)
Cl4	0.2183(2)	0.1426(6)	0.2934(3)	0.0402(11)
N1	0.4857(6)	0.1647(18)	0.7694(8)	0.025(3)
H1	0.5323	0.1185	0.7632	0.030978
N2	0.7892(7)	0.3126(18)	0.0080(8)	0.030(4)
H2	0.802	0.3511	0.0727	0.036622
C1	0.4666(8)	0.283(3)	0.6788(13)	0.042(5)
H1a	0.5001	0.4059	0.6697	0.060187
H1b	0.4181	0.333	0.6851	0.060187
H1c	0.4696	0.1892	0.6204	0.060187
C2	0.4857(9)	0.311(3)	0.8622(11)	0.043(5)
H2a	0.5175	0.4345	0.8513	0.067108
H2b	0.5013	0.2324	0.9217	0.067108
H2c	0.4367	0.3574	0.8739	0.067108
C3	0.4379(8)	−0.023(3)	0.7867(13)	0.042(5)
H3a	0.4517	−0.0947	0.8487	0.06177
H3b	0.4426	−0.1203	0.73	0.06177
H3c	0.389	0.0222	0.7918	0.06177
C4	0.7785(8)	0.510(2)	−0.0501(11)	0.032(4)
H4a	0.8235	0.5955	−0.0538	0.050187
H4b	0.7421	0.5953	−0.0177	0.050187
H4c	0.7627	0.4749	−0.1187	0.050187
C5	0.7204(11)	0.183(3)	0.0119(15)	0.060(7)
H5a	0.7277	0.0553	0.0521	0.098263
H5b	0.7058	0.1435	−0.0556	0.098263
H5c	0.6838	0.268	0.0436	0.098263
C6	0.8479(11)	0.183(3)	−0.0360(14)	0.054(6)
H6a	0.854	0.0579	0.0068	0.079684
H6b	0.8921	0.2697	−0.0373	0.079684
H6c	0.8346	0.1382	−0.1034	0.079684

Table 5
Atomic coordinates and equivalent isotropic thermal parameters for the model M_{C3} at 161 K

	x	y	z	U_{iso} (Å^2)
Hg	0.34402(3)	0.26703(9)	0.25905(4)	0.02662(17)
Cl(1)	0.3428(2)	0.6809(5)	0.2634(3)	0.0308(9)
Cl(2)	0.4019(2)	0.1803(6)	0.0967(3)	0.0329(10)
Cl(3)	0.4311(2)	0.1793(6)	0.3998(2)	0.0293(9)
Cl(4)	0.2183(2)	0.1428(6)	0.2935(3)	0.0404(11)
Trimethylammonium molecular cation				
N(1)	0.0	0.0	0.0	0.028(2)
H(1)	0.0	0.0	0.074	0.051
C(1)	0.0769(4)	0.0	−0.0354(8)	0.071(3)
	φ	χ	ψ	
TrMA(1)	71.3(6)	96.5(5)	−65.8(4)	
TrMA(2)	135.6(14)	21.0(5)	−42.9(14)	
	X_0	Y_0	Z_0	
TrMA(1)	0.4866(5)	0.1661(14)	0.7701(6)	
TrMA(2)	0.7892(4)	0.3115(14)	0.0075(7)	

Standard uncertainties are given in parentheses.

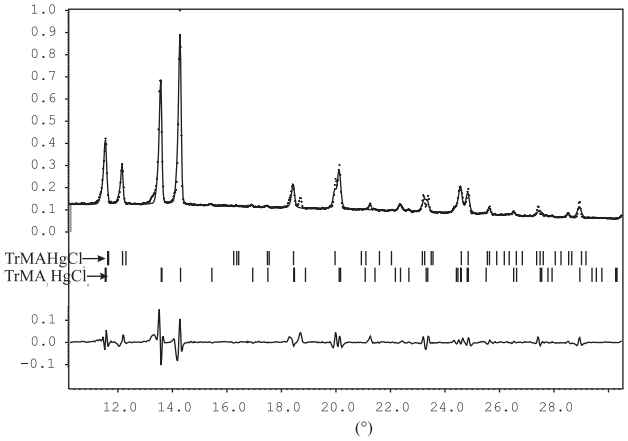

Fig. 6. Scattered intensity of $TrMA_2HgCl_4$ at $T = 373$ K as a function of the diffraction angle. Shown are the observed pattern with the best fit profile (top), the difference curve between observed and calculated profiles (bottom), and the reflection markers with the upper trace corresponding to the impurity phase $TrMA_2HgCl_3$ and the lower trace corresponding to the orthorhombic lattice of $TrMA_2HgCl_4$.

changes in the network of hydrogen bonds. Accordingly, a non-symmetry breaking structural transition was proposed to occur at temperature of 325 K.

Refinements of the structure at 343 K in the model M_{ord} are found to be unstable. The structure parameters of the carbon atoms are highly correlated amongst each other, resulting in physically unreasonably short N–C distances. The origin for these dependencies probably is the much smaller number of observed reflections than could be obtained at room temperature.

3.4. High-temperature X-ray powder diffraction

Indexing of the diffraction data was done with the computer program ITO [20]. The diffraction data at 333 K and below could be described by the expected monoclinic lattice, together with a second lattice for the impurity phase. The data at 343 K and higher temperatures could be indexed with an orthorhombic lattice. Lattice parameters were obtained from LeBail-type fits [21] using the computer program JANA2000 [17]. The peak profile was described by a pseudo-Voigt function, in combination with a special function that accounts for the asymmetry due to axial divergence [22,23]. The lattice was obtained as primitive orthorhombic with $a = 12.279(3)$ Å, $b = 8.767(1)$ Å and $c = 15.139(1)$ Å at $T = 373$ K (Fig. 6). The lattice parameters resemble those of the TMA_2HgCl_4, suggesting that this compound and the high-temperature phase of $TrMA_2HgCl_4$ are isostructural, i.e. they both have the β-K_2SeO_4 structure type. Accordingly, the transition at $\sim$343 K is a $\alpha \leftrightarrow \beta$ phase transition. Due to the low quality of the powder diffraction data, and due to the known non-linearity of the 2θ axis of the INEL detector we did not succeed in a structure solution for the high-temperature phase.

4. MEM analysis

The electron density in the unit cell was studied by the MEM applied to the X-ray data obtained at temperatures of 161, 295 and 343 K, employing the computer program BAYMEM [24]. Experimental structure factors were obtained as the scaled $|F_{obs}|$ data, corrected for anomalous scattering and secondary extinction, together with the phases of F_{calc} of the models M_{C3}. MEM computations using F_{calc} from the best refinements as "experimental" data were performed to test the convergence. In these cases the structure model was reproduced by the MEM. The electron density was discretized on a grid of $128 \times 128 \times 128$ pixels. The entropy was maximized with the χ^2 constraint as boundary condition. Computed structure factors were obtained as the Fourier transform of the trial electron density map. Convergence was defined when χ^2 became less than 1. The final values of the R factors were 0.020 for the 161 K data, 0.028 for the 295 K data and 0.035 for the 343 K data.

The crystal structures were analyzed by studying different sections of the electron density maps as obtained by the MEM optimization: ρ^{161}_{MEM} for the 161 K data, ρ^{295}_{MEM} for the 295 K data, and ρ^{343}_{MEM} for the 343 K data. The sections corresponding to the plane through the atoms Cl(1), Cl(2) and Cl(3) are shown in Fig. 7. The typical shapes of the maxima in these sections indicate the librations of the $HgCl_4$ group are larger than the translations. Sections of ρ^{161}_{MEM}, ρ^{295}_{MEM} and ρ^{343}_{MEM} through the sites of TrMA(1) and TrMA(2)

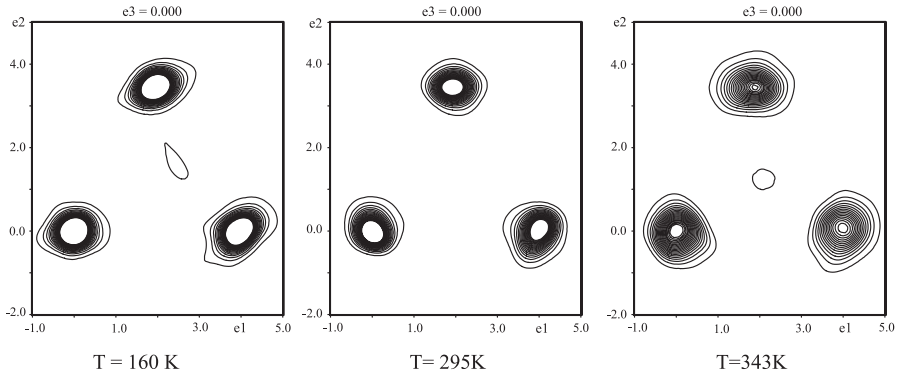

Fig. 7. Sections of the electron densities through the planes defined by the atoms Cl(1), Cl(2) and Cl(3). (a) ρ_{mem}^{161}, (b) ρ_{mem}^{295}, and (c) ρ_{mem}^{343}. Contours are drawn at an interval of 1.0 e/Å^2.

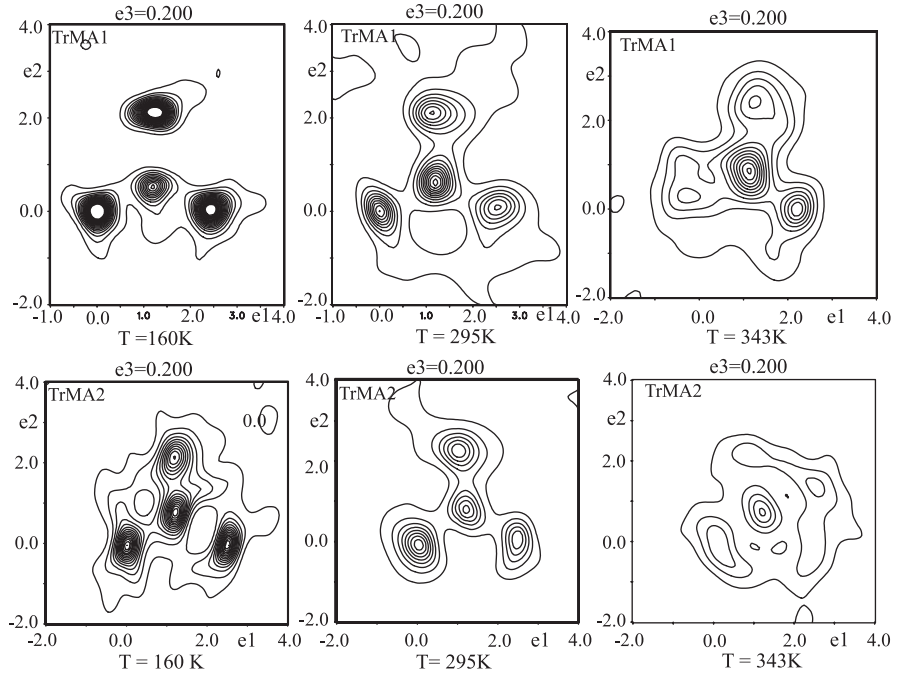

Fig. 8. Sections of the electron densities through the planes defined by three C atoms belonging to single orientations of the $TrMA^+$ cations. ρ_{mem}^{161}, ρ_{mem}^{295} and ρ_{mem}^{343} at the site of TrMA(1), ρ_{mem}^{161}, ρ_{mem}^{295} and ρ_{mem}^{343} at the site of TrMA(2). Contour intervals are 0.1 e/Å^3 with a cut-off at 10 e/Å^3.

clearly show the approximate C3 symmetry of the $TrMA^+$ groups (Fig. 8). The density of the C atoms is more smeared out at higher temperatures than at lower temperatures, suggesting that at 343 K the $TrMA^+$ groups have a higher degree of orientational disorder than at lower temperatures. The weaker localization of the C atoms in TrMA(2) than in TrMA(1) at 343 K is in good agreement with the larger values of the temperature parameters for the TrMA(2) group in the structure refinement at this temperature.

On the basis of the MEM calculations, the phase transition at 325 K can be due to a transition from an ordered state at room temperature towards a state of orientational disorder at higher temperatures. Analysis of the structure then shows that a change of symmetry is not required for this type of modifications of the crystal structure.

5. Discussion

The $HgCl_4^{2-}$ complex anions exhibit a small but definite deviation from tetrahedral symmetry. The major part of this deviation is the spread of bond angles Cl–Hg–Cl that is approximately independent of temperature at 16.3° (Table 6). This deviation is larger than that of $HgCl_4^{2-}$ in TMA_2HgCl_4 (TMA = tetramethylammonium), in accordance with the higher symmetry of the environment of $HgCl_4^{2-}$ in the latter compound [25].

Table 6
Geometry of the $HgCl_4^{2-}$ groups. Bond lengths (Å) and bond angles (deg) are given for three different temperatures

Atoms	$T = 161$ K	$T = 295$ K	$T = 343$ K[a]
Hg–Cl(1)	2.553(3)	2.568(2)	2.604(4)
Hg–Cl(2)	2.441(3)	2.441(1)	2.442(10)
Hg–Cl(3)	2.508(3)	2.481(1)	2.430(7)
Hg–Cl(4)	2.447(4)	2.428(2)	2.414(4)
Cl(1)–Hg–Cl(2)	105.00(11)	104.73(5)	104.1(3)
Cl(1)–Hg–Cl(3)	103.17(11)	103.22(5)	101.4(2)
Cl(1)–Hg–Cl(4)	105.40(12)	104.23(6)	102.7(2)
Cl(2)–Hg–Cl(3)	107.76(11)	109.09(5)	110.9(3)
Cl(2)–Hg–Cl(4)	120.27(13)	119.02(6)	117.5(4)
Cl(3)–Hg–Cl(4)	113.49(13)	114.65(5)	117.3(4)

The results for M_{ord} and M_{C3} are equal within one standard uncertainty.
[a] Data from Ref. [10].

Table 7
Geometry of the $TrMA^+$ molecular cations in the model M_{ord}

Atoms	$T = 161$ K	$T = 295$ K
N(1)–H(1)	0.91	0.91
N(1)–C(1)	1.44(2)	1.458(8)
N(1)–C(2)	1.51(2)	1.452(9)
N(1)–C(3)	1.44(2)	1.478(9)
H(1)–N1–C(1)	109.4(11)	108.2(4)
H(1)–N1–C(2)	106.1(11)	107.9(5)
H(1)–N1–C(3)	108.2(11)	107.6(6)
C(1)–N1–C(2)	110.6(11)	111.4(6)
C(1)–N1–C(3)	112.5(11)	111.2(5)
C(2)–N1–C(3)	109.8(11)	110.5(5)
N(2)–H(2)	0.91	0.91
N(2)–C(4)	1.45(2)	1.456(8)
N(2)–C(5)	1.47(2)	1.443(11)
N(2)–C(6)	1.48(2)	1.484(12)
H(2)–N(2)–C(4)	108.1(11)	107.4(5)
H(2)–N(2)–C(5)	108.7(12)	107.8(6)
H(2)–N(2)–C(6)	108.4(13)	107.3(6)
C(4)–N(2)–C(5)	109.4(12)	111.7(6)
C(4)–N(2)–C(6)	111.8(12)	109.2(5)
C(5)–N(2)–C(6)	110.3(13)	113.1(7)

Bond lengths (Å) and bond angles (deg) are given at two different temperatures.

The $TrMA^+$ molecular cations have been described by two different models: either a free refinement of all atoms (model M_{ord}) or a refinement with restrictions according to an internal 3-fold symmetry (model M_{C3}). Comparison of the geometries of the $TrMA^+$ in the two models shows that the different X-ray data do not contain evidence for a deviation from 3-fold symmetry (Tables 7 and 8). This result is in accordance with the findings for TMA_2HgCl_4, where deviations from tetragonal symmetry of the TMA molecular cations could not be found [25]. The geometry of $TrMA^+$ at 343 K is much less accurately determined than at lower temperatures, as can be explained by the increased orientational disorder of $TrMA^+$ at this temperature (see below).

Table 8
Geometry of the $TrMA^+$ molecular cation in the model M_{C3}

Atoms	$T = 161$ K	$T = 295$ K	$T = 343$ K[a]
N(1)–H(1)	0.97	0.97	0.97
N(1)–C(1)	1.486(13)	1.481(7)	1.42(2)
H(1)–N(1)–C(1)	108.2(9)	107.2(5)	105.0(11)
C(1)–N(1)–C(1)[b]	110.8(8)	111.7(5)	113.5(10)

Bond lengths (Å) and bond angles (deg) are given for three different temperatures.
[a] Data from Ref. [10].
[b] Obtained by application of the 3-fold axis to C(1).

The interactions between $HgCl_4^{2-}$ and $TrMA^+$ involve direct Coulomb interactions and hydrogen bonds. Weak hydrogen bonds of the type N–H···Cl (distance H···Cl less than 2.6 Å) are found between both independent $TrMA^+$ cations and Cl(1). The strengths of these bonds is very similar at 161 and 295 K (Table 9). Weak hydrogen bonds of the type C–H···Cl (distance C···Cl less than 2.9 Å) involve the Cl(1), Cl(2) and Cl(3) atoms. Both at 161 and at 295 K several of these contacts are present, although they differ in strength and in some cases one contact has been replaced by another. Many more contacts can be identified when distances C···Cl around 3.0 Å are also considered, but these interactions most probably are too weak to be considered hydrogen bonds. Weak hydrogen bonds N–H···Cl and C–H···Cl have been studied before in related compounds by Taylor [26] and Hitchcock et al. [27] (also see [8]). The present results show that weak hydrogen bonds are essential to understand the stability of $TrMA_2HgCl_4$. Previously, we have determined that the structure at 343 K possesses a different arrangement of hydrogen bonds [10], and the transition at ~325 K is related to changes in the network of hydrogen bonds (see below).

The DSC experiment indicates four phase transitions to occur between 230 and 360 K (Fig. 1). The largest anomaly in the DSC (with a large hysteresis) was identified by X-ray powder diffraction as a first-order phase transition between the α and β forms of the K_2SeO_4 structure type (Fig. 3). The transition temperature on heating was determined as ~350 K.

The second-largest anomaly in the DSC occurs at ~325 K. Previously we have shown that the a lattice parameter exhibits an anomalously large increase between 310 and 330 K [10]. Furthermore the structure at 343 K has a different pattern of hydrogen bonds than the room temperature structure. This has lead us to interpret the transition at ~325 K as a continuous structural change in a narrow temperature interval. The previous refinements were restricted to an ordered structure. Presently, we have determined the electron density by the MEM. The density at the sites of the $TrMA^+$ molecular cations shows, that the orientational disorder of these ions is much larger at 343 K than it is

Table 9
Hydrogen-bonds at 161 and 295 K in the model M_{ord}

D–H···Cl	D–H	H···Cl	D···Cl	D–H···Cl
Temperature = 295 K				
N(1)–H(1)···Cl(1)^{ii}	0.91	2.573(2)	3.274(5)	134.8(4)
N(2)–H(2)···Cl(1)^{iv}	0.91	2.494(1)	3.246(5)	140.9(3)
C(1)–H(1a)···Cl(3)^{ii}	0.96	2.964(1)	3.899(7)	164.1(4)
C(1)–H(1b)···Cl(4)^{iii}	0.96	2.942(2)	3.807(7)	150.7(4)
C(1)–H(1c)···Cl(3)	0.95	2.970(1)	3.726(6)	137.2(4)
C(1)–H(1c)···Cl(3)^{i}	0.95	3.059(2)	3.703(7)	126.2(4)
C(2)–H(2a)···Cl(2)^{v}	0.96	2.963(1)	3.576(7)	122.9(4)
C(2)–H(2b)···Cl(4)^{iii}	0.96	3.048(2)	3.889(8)	147.5(4)
C(2)–H(2c)···Cl(2)^{ii}	0.95	2.889(2)	3.780(8)	155.9(4)
C(3)–H(3a)···Cl(2)^{i}	0.96	2.909(2)	3.539(8)	124.0(5)
C(3)–H(3b)···Cl(3)^{i}	0.96	2.905(1)	3.605(8)	131.0(5)
C(3)–H(3c)···Cl(4)^{iii}	0.95	2.913(2)	3.778(8)	151.7(5)
C(4)–H(4a)···Cl(3)^{iii}	0.95	2.881(2)	3.529(7)	126.8(4)
C(4)–H(4b)···Cl(4)^{iii}	0.96	3.057(2)	3.753(7)	130.7(4)
C(4)–H(4c)···Cl(1)^{vi}	0.98	2.790(1)	3.728(7)	161.8(4)
C(5)–H(5c)···Cl(2)^{vii}	0.96	2.786(2)	3.493(10)	131.0(6)
C(6)–H(6c)···Cl(3)^{iv}	0.96	2.986(2)	3.895(10)	157.7(7)
Temperature = 161 K				
N(1)–H(1)···Cl(1)^{ii}	0.92	2.589(3)	3.285(11)	133.3(7)
N(1)–H(1)···Cl(2)^{i}	0.92	2.893(4)	3.489(11)	124.0(7)
N(1)–H(1)···Cl(3)^{i}	0.92	2.908(3)	3.460(11)	120.1(7)
N(2)–H(2)···Cl(1)^{iv}	0.92	2.511(3)	3.257(12)	139.8(7)
N(2)–H(2)···Cl(4)^{iii}	0.92	2.976(4)	3.572(12)	124.8(8)
C(1)–H(1a)···Cl(3)^{ii}	0.96	2.953(3)	3.885(16)	163.1(10)
C(1)–H(1b)···Cl(4)^{iii}	0.96	2.886(4)	3.754(16)	151.6(10)
C(1)–H(1c)···Cl(3)	0.96	2.969(3)	3.755(17)	139.8(10)
C(1)–H(1c)···Cl(3)^{i}	0.96	2.978(4)	3.623(17)	125.6(9)
C(2)–H(2a)···Cl(2)^{ii}	0.95	2.835(4)	3.729(17)	156.8(9)
C(2)–H(2b)···Cl(2)^{v}	0.97	2.937(3)	3.510(15)	119.1(10)
C(3)–H(3a)···Cl(2)^{i}	0.96	2.849(4)	3.483(16)	124.2(9)
C(3)–H(3b)···Cl(3)^{i}	0.96	2.908(3)	3.584(16)	128.3(9)
C(3)–H(3c)···Cl(4)^{iii}	0.95	2.908(4)	3.770(16)	151.4(10)
C(4)–H(4a)···Cl(3)^{iii}	0.97	2.853(3)	3.546(15)	151.5(9)
C(4)–H(4b)···Cl(4)^{iii}	0.97	2.979(4)	3.636(15)	126.4(8)
C(4)–H(4c)···Cl(1)^{vi}	0.96	2.849(3)	3.731(14)	152.6(8)
C(5)–H(5b)···Cl(2)^{vii}	0.95	2.809(4)	3.42(2)	122.9(12)
C(6)–H(6a)···Cl(3)^{iii}	0.96	3.028(3)	3.93(2)	157.4(12)

Distances (Å) D–H, H···Cl and D···Cl, and the angle (deg) D–H···Cl are shown for each hydrogen bond D–H···Cl with D equal to N or C. Symmetry codes $^{i}1-x,-y,1-z$; $^{ii}1-x,1-y,1-z$; $^{iii}1/2+x,1/2+y,1/2-z$; $^{iv}1/2+x,-1/2+y,1/2-z$; $^{v}-x,-y,1-z$; $^{vi}1-x,1-y,-z$; $^{vii}1-x,-y,-z$.

at 295 K (Fig. 8). This effect is more pronounced for TrMA(2) than for TrMA(1), and it suggests that above ~325 K the TrMA(2) exhibits a high degree of orientational disorder. This interpretation is supported by the refinements, which give larger temperature parameters for TrMA(2) than for TrMA(1). Consequently, instead of assigning a different pattern of hydrogen bonds to the structure between 325 and 350 K, the present results suggest that this phase is characterized by a dynamical, orientational disorder of TrMA(2), with rotations of this molecular ion about the N–H axis.

DSC indicates two further phase transitions to occur at or below room temperature. However, the smooth thermal expansion (Fig. 6) and the great similarities between the structures at 161 and 295 K (Tables 6, 7 and 9) both indicate the absence of a structural phase transition below room temperature. For example, we did not obtain any evidence for rotations of the organic cations as they have been identified to occur in dimethylammonium-$CoCl_4$ between room temperature and 235 K [5]. In agreement with the X-ray diffraction results, NMR does not give any evidence for a phase transition at low temperatures (Fig. 4). So, on the basis of the present experimental results we can exclude a structural origin for the transitions below room temperature, but we have not been able to definitely establish their existence or to uncover their mechanism.

6. Conclusions

DSC experiments indicate four phase transition in $TrMA_2HgCl_4$ to occur between 230 and 350 K. One first-order phase transition occurs at ~350 K, that was identified as a transition between the α and β forms of the K_2SeO_4 structure type, on the basis of X-ray powder diffraction. Complete crystal structures have been determined at temperatures of 161, 295 and 343 K. They show that a second transition at ~325 K most probably is a continuous structural change in a narrow temperature interval, that amounts to a transition between ordered $TrMA^+$ cations at room temperature and rotating $TrMA^+$ cations above 325 K. A structural component could not be found for the two other transitions in the DSC. This interpretation is in complete agreement with the observations by temperature dependent NMR.

Structure refinements have been performed, employing alternatively the full space group symmetry and additional restrictions on the $TrMA^+$ ions by local 3-fold axes. The comparison of these models has shown that the $TrMA^+$ ions do have 3-fold symmetry at all temperatures. The $HgCl_4^{2-}$ ions have small but definite deviations from tetrahedral symmetry, that is of similar size at all temperatures. The distortion of these anions is larger than in TMA_2HgCl_4, as can be understood from the less symmetric environment of $HgCl_4^{2-}$ in $TrMA_2HgCl_4$.

Acknowledgments

Financial support was obtained from the DAAD (Germany).

References

[1] G.D. Stucky, J.B. Folker, T.J. Kistenmacher, Acta Crystallogr. 23 (1967) 1067–1070.

[2] I.D. Williams, P.W. Brown, N.J. Taylor, Acta Crystallogr. C 48 (1992) 259–263.
[3] A. Mahoui, J. Lapasset, J. Moret, P. Saint Gregoire, Acta Crystallogr. C 52 (1996) 2671–2674.
[4] A. Mahoui, J. Lapasset, J. Moret, P. Saint Gregoire, Acta Crystallogr. C 52 (1996) 2674–2676.
[5] I.D. Williams, P.W. Brown, N.J. Taylor, Acta Crystallogr. C 48 (1992) 263–266.
[6] C.B. Aakeröy, T.A. Evans, K.R. Seddon, I. Palinko, New J. Chem. 2 (1999) 145–152.
[7] F.H. Allen, O. Kennard, Chem. Des. Autom. News 8 (1993) 31–37.
[8] G.R. Desiraju, Th. Steiner, The Weak Hydrogen Bond, Oxford University Press, Oxford, UK, 1999.
[9] A. Ben Salah, J.W. Bats, H. Fuess, A. Daoud, Z. Kristallogr. 164 (1983) 259–272.
[10] M. Amami, S. van Smaalen, A. Ben Salah, Acta Crystallogr. E 58 (2002) m416–m419.
[11] C.J. Gilmore, Acta Crystallogr. A 52 (1996) 561–589.
[12] A.L. Spek, A. Meetsma, HELENA, University of Groningen, The Netherlands.
[13] W. Herrendorf, Ph.D. Thesis, University of Karlsruhe, Germany, 1992.
[14] Siemens, SMART and SAINT, Siemens Analytical X-ray Instruments Inc., Madison, WI, USA, 1995.
[15] G.M. Sheldrick, SADABS, University of Göttingen, Germany, 1996.
[16] G.M. Sheldrick, SHELXS97 and SHELXL97, University of Göttingen, Germany, 1996.
[17] V. Petricek, M. Dusek, The Crystallographic Computing System JANA2000, Institute of physics of the Academy of Sciences, Praha, 2000.
[18] R.E. Dinnebier, U. Behrens, F. Olbrich, J. Amer. Chem. Soc. 120 (1998) 1430–1433.
[19] E.O. Stejskal, J.D. Memory, High Resolution NMR in the Solid State, Oxford University Press, New York, 1994.
[20] J.W. Visser, J. Appl. Crystallogr. 2 (1969) 89–95.
[21] A. Lebail, H. Duroy, J.L. Fourquet, Mater. Res. Bull. 23 (1988) 447–452.
[22] P. Thompson, D.E. Cox, J.B. Hastings, J. Appl. Crystallogr. 20 (1987) 79–83.
[23] L.W. Finger, D.E. Cox, A.P. Jephcoat, J. Appl. Crystallogr. 27 (1994) 892–900.
[24] S. van Smaalen, L. Palatinus, M. Schneider, Acta Crystallogr. A 59 (2003) 459–469.
[25] M. Amami, S. van Smaalen, L. Palatinus, A. Ben Salah, X. Helluy, A. Sebald, Z. Kristallogr. 217 (2002) 532–541.
[26] R. Taylor, O. Kennard, J. Amer. Chem. Soc. 104 (1982) 5063–5070.
[27] P.B. Hitchcock, K.R. Seddon, T.J. Welton, Chem. Soc. Dalton Trans. (1993) 2639–2643.